Fermilab FERMILAB-Conf-02/367-A January 2003

SUPERNOVA NEUTRINOS

J. F. BEACOM
NASA/Fermilab Astrophysics Center, Fermi National Accelerator Laboratory, Batavia, Illinois 60510-0500, USA
E-mail: beacom@fnal.gov

We propose that neutrino-proton elastic scattering, $\nu + p \to \nu + p$, can be used for the detection of supernova neutrinos. Though the proton recoil kinetic energy spectrum is soft, with $T_p \simeq 2E_\nu^2/M_p$, and the scintillation light output from slow, heavily ionizing protons is quenched, the yield above a realistic threshold is nearly as large as that from $\bar{\nu}_e + p \to e^+ + n$. In addition, the measured proton spectrum is related to the incident neutrino spectrum, which solves a long-standing problem of how to separately measure the total energy release and temperature of ν_μ, ν_τ, $\bar{\nu}_\mu$, and $\bar{\nu}_\tau$. The ability to detect this signal would give detectors like KamLAND and Borexino a crucial and unique role in the quest to detect supernova neutrinos.

1 Introduction

When the next Galactic supernova comes, will we have enough information to study the supernova neutrino signal in detail? Almost all of the detected events will be charged-current $\bar{\nu}_e + p \to e^+ + n$, which will be well-measured, both because of the large yield and because the measured positron spectrum is related to the neutrino spectrum. Because of the charged-lepton thresholds, the flavors ν_μ, ν_τ, $\bar{\nu}_\mu$, and $\bar{\nu}_\tau$ can only be detected in neutral-current reactions, of which the total yield is expected to be approximately 10^3 events. However, as will be discussed below, in general one *cannot* measure the neutrino energy in neutral-current reactions. These four flavors are expected to carry away about 2/3 of the supernova binding energy, and are expected to have a higher temperature than ν_e or $\bar{\nu}_e$. However, there is no experimental basis for these statements, and at present, numerical models of supernovae cannot definitively address these issues either. If there is no spectral signature for the detection reactions, then neither the total energy carried by these flavors nor their temperature can be separately determined from the detected number of events.

For example, the total energy is needed to determine the mass of the neutron star, and the temperature is needed for studies of neutrino oscillations. At present, such studies would suffer from the need to make model-dependent assumptions. This problem has long been known, but perhaps not widely enough appreciated. In Ref.[1], we clarify this problem, and provide a realistic solution that can be implemented in two existing detectors, KamLAND and

Borexino. The solution is based on neutrino-proton elastic scattering, which has been observed at accelerators at GeV energies, but has never before been shown to be a realistic detection channel for low-energy neutrinos.

2 Main Ideas

If all terms of order E_ν/M_p or higher powers are neglected, the differential cross section for $\nu + p \to \nu + p$ is very simple:

$$\frac{d\sigma}{dT_p} = \frac{G_F^2 M_p}{\pi}\left[\left(1 - \frac{M_p T_p}{E_\nu^2}\right) c_V^2 + \left(1 + \frac{M_p T_p}{E_\nu^2}\right) c_A^2\right] . \tag{1}$$

The neutral-current coupling constants between the exchanged Z° and the proton are

$$c_V = \frac{1 - 4\sin^2\theta_w}{2} = 0.04 \tag{2}$$

$$c_A = \frac{1.27}{2} , \tag{3}$$

where the factor 1.27 is determined by neutron beta decay and its difference from unity is a consequence of the partially conserved axial current. Since $c_A \gg c_V$, this form makes it clear that the *largest* proton recoils are favored, which is optimal for detection. Note that this is the *opposite* behavior compared to neutrino-electron elastic scattering, where both the vector and axial couplings contribute, and where E_ν/m_e is not small. It also means that the neutrino (c_A) and antineutrino ($-c_A$) cross sections are nearly identical. If c_V is neglected and the differential cross section is expressed in terms of $\cos\theta_\nu$, it follows the form $1 - 1/3\cos\theta_\nu$ expected for a non-relativistic axial coupling (i.e., a Gamow-Teller matrix element). The total cross section is

$$\frac{G_F^2 E_\nu^2}{\pi}\left(c_V^2 + 3c_A^2\right) . \tag{4}$$

As expected, this is of the same form as the total cross section for the charged-current reaction $\bar{\nu}_e + p \to e^+ + n$. However, note that the vector coupling nearly vanishes in the neutral-current channel, and that the axial coupling is half as large as in the charged-current channel, thus making the total cross section approximately 4 times smaller. This factor of 4 can be immediately obtained by considering the product of the couplings and the propagator factor, and using the definition of θ_W. However, for a supernova, several flavors contribute to the neutral-current signal.

The supernova binding energy release about 3×10^{53} ergs, about 99% of which is carried off by all flavors of neutrinos and antineutrinos over about

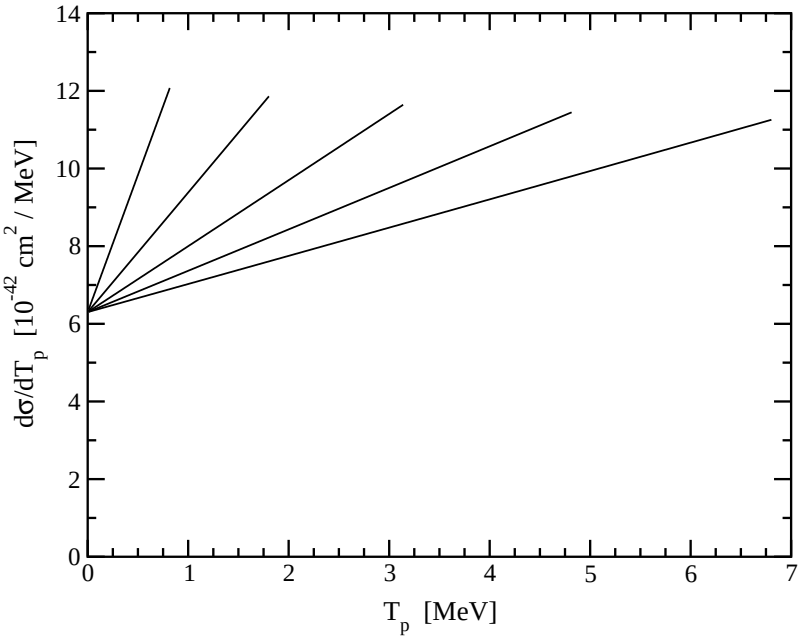

Figure 1. The differential cross section as a function of T_p for fixed E_ν. Note the rise at large T_p, indicating that high recoil energy is preferred. From left to right, the lines are for $E_\nu = 20, 30, 40, 50,$ and 60 MeV.

10 s. The emission time is much longer than the light-crossing time of the proto-neutron star because the neutrinos are trapped and must diffuse out, eventually escaping with approximately Fermi-Dirac spectra characteristic of the surface of last scattering. In the canonical model, ν_μ, ν_τ and their antiparticles have a temperature $T \simeq 8$ MeV, $\bar{\nu}_e$ has $T \simeq 5$ MeV, and ν_e has $T \simeq 3.5$ MeV. The temperatures differ from each other because $\bar{\nu}_e$ and ν_e have charged-current opacities (in addition to the neutral-current opacities common to all flavors), and because the proto-neutron star has more neutrons than protons. It is generally assumed that each of the six types of neutrino and antineutrino carries away about 1/6 of the total binding energy, though this has an uncertainty of at least 50%.

Elastically-scattered protons will have kinetic energies of a few MeV. Obviously, these very nonrelativistic protons will be completely invisible in any Čerenkov detector like Super-Kamiokande. However, such small energy de-

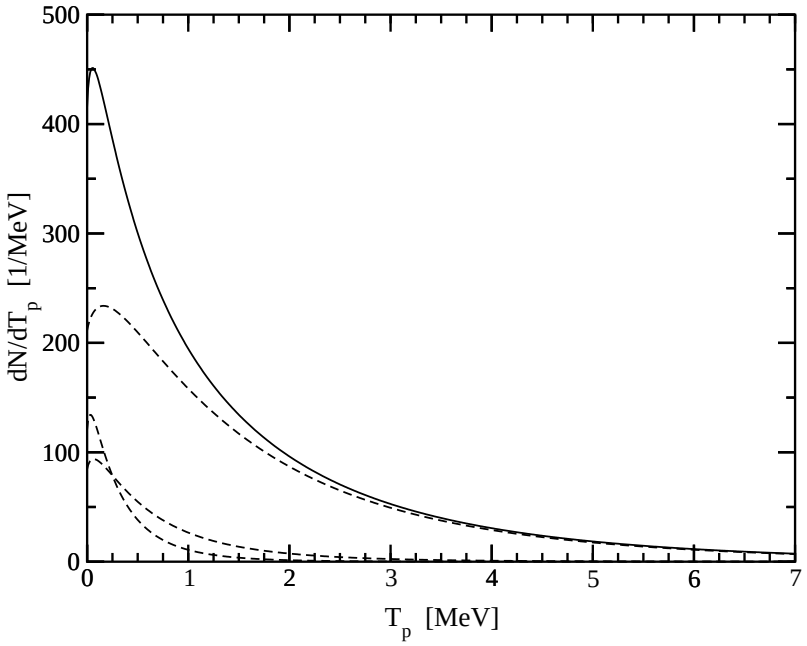

Figure 2. The true proton spectrum in KamLAND, for a standard supernova at 10 kpc. In order of increasing maximum kinetic energy, the contributions from ν_e, $\bar{\nu}_e$, and the sum of ν_μ, ν_τ, $\bar{\nu}_\mu$, and $\bar{\nu}_\tau$ are shown with dashed lines. The solid line is the sum spectrum for all flavors. Taking the detector properties into account substantially modifies these results, as shown below.

positions can be readily detected in scintillator detectors such as KamLAND and Borexino. We first consider the true proton spectrum, and then we consider how this spectrum would appear in a realistic detector. The true proton spectrum is given by

$$\frac{dN}{dT_p}(T_p) = C \int_{(E_\nu)_{min}}^{\infty} dE_\nu \, f(E_\nu) \, \frac{d\sigma}{dT_p}(E_\nu, T_p) \,, \tag{5}$$

where $f(E_\nu)$ is a normalized Fermi-Dirac spectrum and the differential cross section is given above. For a given T_p, the minimum required neutrino energy is

$$(E_\nu)_{min} = \frac{T_p + \sqrt{T_p(T_p + 2M_p)}}{2} \simeq \sqrt{\frac{M_p T_p}{2}} \,. \tag{6}$$

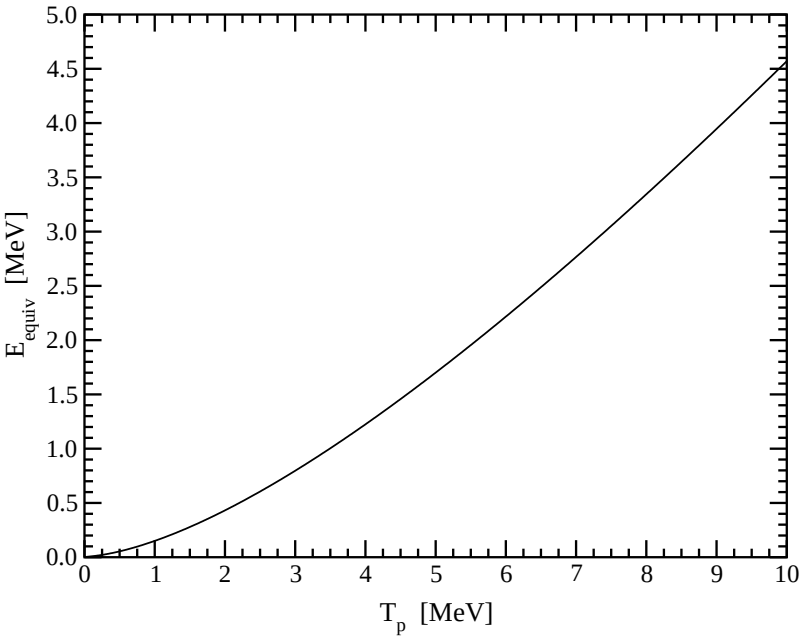

Figure 3. The quenched energy deposit (equivalent electron energy) as a function of the proton kinetic energy. The KamLAND detector properties are assumed.

For highly ionizing particles like low-energy protons, the light output is reduced or "quenched" relative to the light output for an electron depositing the same amount of energy. The observable light output E_{equiv} (i.e., equivalent to an electron of energy E_{equiv}) is given by Birk's Law:

$$\frac{dE_{equiv}}{dx} = \frac{dE/dx}{1 + k_B(dE/dx)} \tag{7}$$

where k_B is a constant of the scintillation material, and dE/dx is the energy deposition rate, now in MeV/cm (of opposite sign to the loss rate). We assume $k_B \simeq 0.015$ cm/MeV for KamLAND. For small dE/dx, the measured light output of a proton is equivalent to an electron of the same energy. But for $dE/dx \sim 100$ MeV/cm, the two terms in the denominator are comparable, and the light output is reduced. At still higher dE/dx, then dE_{equiv}/dx tends to a constant. Birk's Law can thus reflects a saturation effect: once dE/dx is large, making it larger does not increase the light output. Effectively, if all

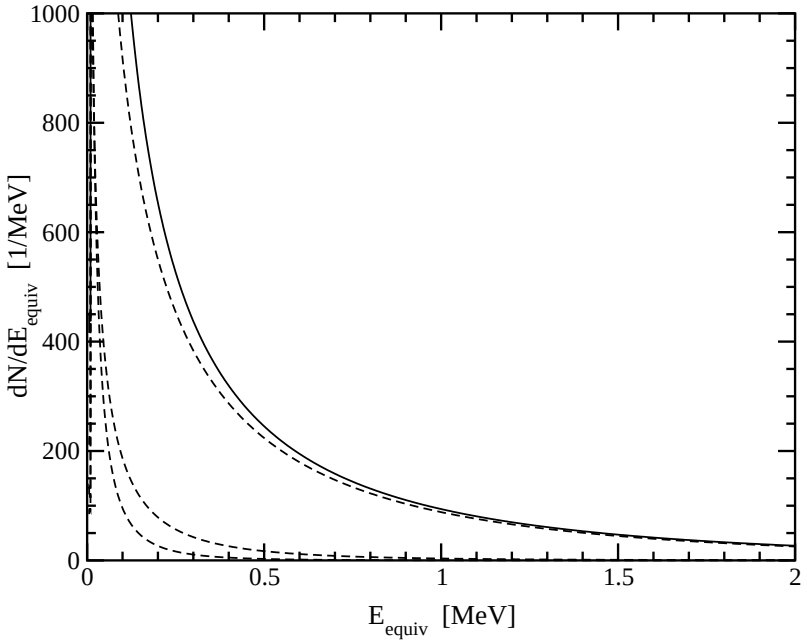

Figure 4. The struck proton spectrum for the different flavors, with quenching effects taken into account. In order of increasing maximum kinetic energy, the contributions from ν_e, $\bar{\nu}_e$, and the sum of ν_μ, ν_τ, $\bar{\nu}_\mu$, and $\bar{\nu}_\tau$ are shown with dashed lines. The solid line is the sum spectrum for all flavors. The anticipated KamLAND threshold is 0.2 MeV electron equivalent energy.

scintillation molecules are already excited, any further energy deposition is not converted to visible scintillation light.

The measured proton spectrum can be used to separately determine the total flux of ν_μ, ν_τ, $\bar{\nu}_\mu$, and $\bar{\nu}_\tau$ neutrinos *and* their time-averaged temperature. The total number of detected events is proportional to the portion of the total binding energy carried away by these four flavors, and we denote this by $E^{tot}_{4\nu_x}$. We do not have to assume that it is equal to $4(E_B/6) = 2/3E_B \simeq 2 \times 10^{53}$ ergs; it can be measured. We denote the temperature of these four flavors by T. If only the total yield were measured, as for most neutral-current reactions, there would be an unresolved degeneracy between $E^{tot}_{4\nu_x}$ and T, since

$$N \sim E^{tot}_{4\nu_x} \frac{\langle\sigma\rangle}{T_\nu} \,. \tag{8}$$

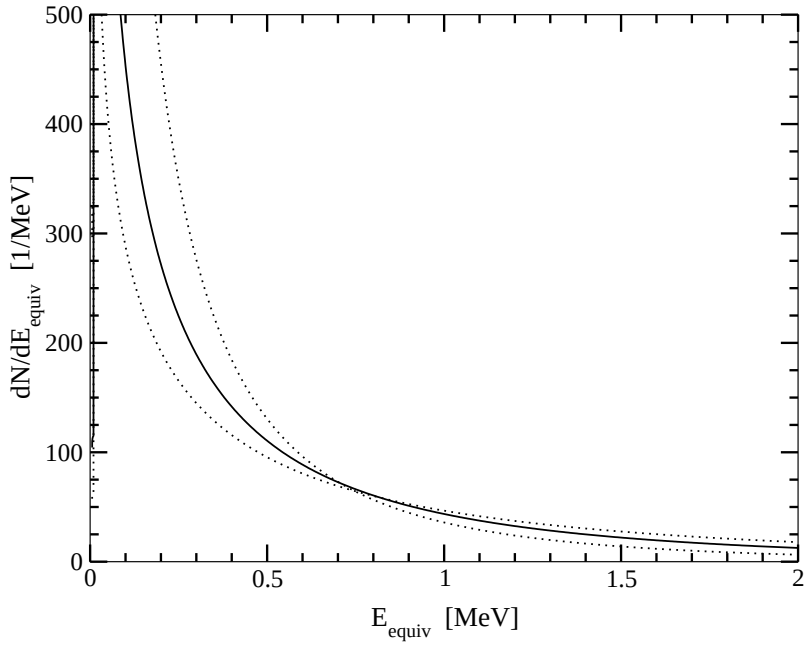

Figure 5. Example spectra with different values of $E^{tot}_{4\nu_x}$ and T, all chosen to give the *same* number of events above an electron equivalent threshold of 0.2 MeV (true proton energy 1.2 MeV). At the 0.2 MeV point, from left to right these correspond to $(E^{tot}_{4\nu_x}, T) = (4.2, 6)$, $(2.0, 8)$, $(1.4, 10)$, respectively, with $E^{tot}_{4\nu_x}$ in 10^{53} ergs and T in MeV.

Note that for $\sigma \sim E^n_\nu$, then $\langle\sigma\rangle \sim T^n$. For $\nu + d \to \nu + p + n$ in SNO, for example, $\sigma \sim E^2$, so $N \sim E^{tot}_{4\nu_x} T$. Thus for a given measured number of events, one would only be able to define a hyperbola in the plane of $E^{tot}_{4\nu_x}$ and T. The scaling is less simple here because of threshold effects, but the idea is the same.

Here we have crucial information on the shape of the neutrino spectrum, revealed through the proton spectrum. To remind the reader, in most neutral-current reactions there is *no* information on the neutrino energy, e.g., one only counts the numbers of thermalized neutron captures, or measures nuclear gamma rays (the energies of which depend only on nuclear level splittings). Neutrino-electron scattering is an exception. However, the distribution of electron energies for a given neutrino energy is very broad, and the electron angle can only be measured to about 25 degrees, which is too large to adequately

Neutrino Spectrum	$E_{thr} = 0$	0.2 MeV
$\nu : T = 3.5$ MeV	57	3
$\bar{\nu} : T = 5$ MeV	80	17
$2\nu : T = 8$ MeV	244	127
$2\bar{\nu} : T = 8$ MeV	243	126
All	624	273

Table 1. Numbers of events in KamLAND above the noted thresholds for a standard supernova at 10 kpc, for the separate flavors or their equivalents. Oscillations do not change the number of neutrinos at a given energy, and the neutral-current yields are insensitive to the neutrino flavor. Equipartition among the six flavors is assumed (see the text for discussion). The thresholds are in electron equivalent energy, and correspond to minimum true proton kinetic energies of 0 and 1.2 MeV.

reconstruct the incident neutrino energy. Also, the scattered electrons, even those in the forward cone, sit on a much larger background of $\bar{\nu}_e + p \rightarrow e^+ + n$ events.

We performed Monte Carlo simulations of the supernova signal in KamLAND and made chi-squared fits to determine $E^{tot}_{4\nu_x}$ and T for each fake supernova.

Three examples are shown in Fig. 6, where one can see that $E^{tot}_{4\nu_x}$ and T_ν can each be determined with roughly 10% error. These errors scale as $1/\sqrt{N}$, where N is the total number of events (i.e., if one imagines a detector of a different mass or a different assumed supernova distance). If the distance were completely uncertain, one would not be able to determine $E^{tot}_{4\nu_x}$. However, after marginalizing over the unknown $E^{tot}_{4\nu_x}$ (i.e., projecting these scatterplots onto the T axis), one would still obtain a good measurement of T.

3 Conclusions

It is important to note that the detection of recoil protons from *neutron*-proton elastic scattering at several MeV has been routinely accomplished in scintillator detectors. Since both particles are massive, the proton will typically take half of the neutron energy. This reaction provides protons in the same energy range as those struck in neutrino-proton elastic scattering with $E_\nu \sim 30$ MeV. This is an important proof of concept for all aspects of the detection of low-energy protons.

Though low-energy backgrounds will be challenging, it is also important to note that the background requirements for detecting the supernova signal are approximately 3 orders of magnitude *less* stringent than those required

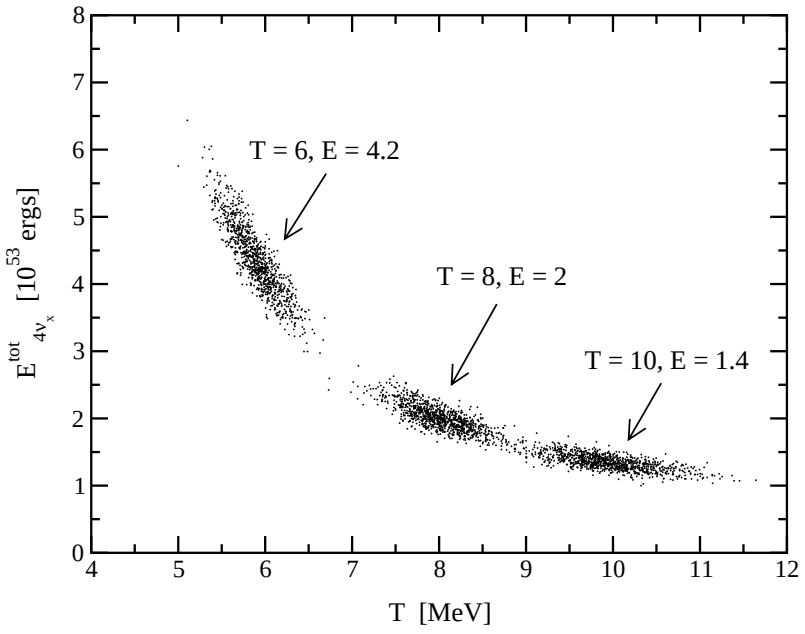

Figure 6. Scatterplot of 10^3 fitted values, in the $E^{tot}_{4\nu_x}$ and T_ν plane, for the labeled "true" values, where $E^{tot}_{4\nu_x}$ is the total portion of the binding energy carried away by the sum of ν_μ, ν_τ, $\bar{\nu}_\mu$, and $\bar{\nu}_\tau$, and T is their temperature. The values of $E^{tot}_{4\nu_x}$ and T_ν were chosen such that the numbers of events above threshold were the same. The measured shape of the proton spectrum breaks the degeneracy between these two parameters. Without that spectral information, one could not distinguish between combinations of $E^{tot}_{4\nu_x}$ and T_ν along the band in this plane that our three examples regions lie along.

for detecting solar neutrinos in the same energy range (taking quenching into account for our signal). Borexino has been designed to detect very low-energy solar neutrinos, and KamLAND hopes to do so in a later phase of their experiment.

We have shown that neutrino-proton elastic scattering, previously unrecognized as a useful detection reaction for low-energy neutrinos, in fact has a yield comparable to $\bar{\nu}_e + p \rightarrow e^+ + n$, even after taking into account the quenching of the proton scintillation light and assuming a realistic detector threshold.

In addition, the measured proton spectrum shape is closely related to the incident neutrino spectrum. We have shown explicitly that one can sepa-

rately measure the total energy release and temperature of ν_μ, ν_τ, $\bar{\nu}_\mu$, and $\bar{\nu}_\tau$, each with uncertainty of order 10%. This greatly enhances the importance of detectors like KamLAND and Borexino for detecting supernova neutrinos.

These measurements would be considered in combination with similar measurements for ν_e and $\bar{\nu}_e$ from charged-current reactions in other detectors. These separate measurements of the total energy release and temperature for each flavor will be invaluable for comparing to numerical supernova models. They will also be required to make model-independent studies of the effects of neutrino oscillations. If the total energy release E_B in all flavors has been measured, then

$$E_B \simeq \frac{3}{5}\frac{GM_{NS}^2}{R_{NS}}\,, \tag{9}$$

thus allowing a direct measurement of the newly-formed neutron star properties.

Acknowledgments

I thank many people for discussions; see Ref. [1]. In particular, my collaborators on Ref. [1], Will Farr and Petr Vogel. JFB was supported as a Sherman Fairchild Fellow at Caltech during the initial part of this project, and as the David N. Schramm Fellow at Fermilab during the final part. Fermilab is operated by URA under DOE contract No. DE-AC02-76CH03000. JFB was additionally supported by NASA under NAG5-10842.

References

1. J.F. Beacom, W.M. Farr, and P. Vogel, in a paper to appear on www.arxiv.org in mid-May 2002.
2. Since space is limited, all references can be found in Ref. [1].